Proceedings of the
1999 ASME Design Engineering Technical Conferences
September 12-15, 1999, Las Vegas, Nevada, USA

DETC99/VIB-8063

SOME NONLINEAR EFFECTS OF MAGNETIC BEARINGS

Norbert Steinschaden
Institute for Machine Dynamics and Measurements
Vienna University of Technology
Wiedner Hauptstraße 8-10 / E303
A-1040 Vienna
Austria
Email: norbert.steinschaden@tuwien.ac.at

Helmut Springer
Institute for Machine Dynamics and Measurements
Vienna University of Technology
Wiedner Hauptstraße 8-10 / E303
A-1040 Vienna
Austria
Email: helmut.springer@tuwien.ac.at

ABSTRACT

In order to get a better understanding of the dynamics of active magnetic bearing (AMB) systems under extreme operating conditions a simple, nonlinear model for a radial AMB system is investigated. Instead of the common way of linearizing the magnetic forces at the center position of the rotor with respect to rotor displacement and coil current, the fully nonlinear force to displacement and the force to current characteristics are used.

The AMB system is excited by unbalance forces of the rotor. Especially for the case of large rotor eccentricities, causing large rotor displacements, the behaviour of the system is discussed. A path-following analysis of the equations of motion shows that for some combinations of parameters well-known nonlinear phenomena may occur, as, for example, symmetry breaking, period doubling and even regions of global instability can be observed.

INTRODUCTION

AMBs represent modern mechatronical systems. The avoidance of any lubrication systems and lubricants, the absence of material wear and almost no friction losses, as a consequence of no mechanical or fluidic contact between the rotor and the stator, are significant advantages resulting in high life time and low maintenance requirements, see (Schweitzer, et al., 1993). If magnetic bearings are used, no additional equipment will be needed for diagnosis and permanent monitoring tasks during machine operation. Stiffness, damping and force characteristics of the bearing can be adapted to actual machine operating conditions by adaptive control strategies easily to be implemented into the feedback control device, see (Lang, et al., 1995). As the area of industrial applications of AMB systems grows, there is a growing demand of highly reliable systems at any operating conditions. This requires a deep and complete understanding of the dynamics of rotor AMB systems.

For a rigid rotor, supported by two lubricated journal bearings, Moser has investigated the nonlinear stability and bifurcation behaviour in terms of three important dimensionless bifurcation parameters, (Moser, 1993). They correspond to the rotor speed, the static load and the unbalance eccentricity of the rotor. For magnetic bearings, there are only a few papers available that partially deal with the problem of nonlinear modeling, stability and bifurcation. Hebbale investigated a four-magnet AMB system with linear state variable control and pole placement design, (Hebbale, 1985; Hebbale, Taylor, 1986). A two degrees of freedom single-mass rotor with nonlaminated (solid) ferromagnetic flux paths was considered which generates speed dependent eddy current effects due to rotation of the rotor. By applying center manifold theory, see (Troger, Steindl, 1991), a subcritical Hopf bifurcation was detected in terms of the rotor speed as the bifurcation parameter. Furthermore, in (Hebbale, 1985; Hebbale, Taylor, 1986) the influence of rotor unbalance on the stability was investigated by numerical simulation studies.

Mohamed and Emad investigated a rigid rotor in two radial AMBs with a linear state variable voltage controller, (Mohamed, Emad, 1993). Nonlinear force to magnetic flux relationships were considered along with speed dependent gyroscopic effects

of the rotor. A subcritical Hopf bifurcation was found for a static equilibrium state in terms of the rotor speed as the distinguished bifurcation parameter.

Wang et al. investigated a single-mass rotor (with and without unbalance) supported by an AMB with linear voltage PD-controller, (Wang, et al., 1994). They considered nonlinear force to air gap and nonlinear force to coil current characteristics. Applying the center manifold theory, bifurcations were found in terms of the controller feedback gain parameters.

Ecker, Knight and Virgin found pitchfork and torus bifurcations for the vibrational amplitudes of an AMB-supported single-mass rotor with unbalance excitation in terms of the rotor speed as the distinguished bifurcation parameter, (Ecker, et al., 1997; Knight, Ecker, 1996; Virgin, et al., 1994). Since they used flux control with a linear feedback law, the only nonlinearities causing the investigated phenomena were nonlinear, conservative cross coupling forces between two pairs of orthogonal oriented electromagnets, see (Knight, et al., 1993; Knight, et al., 1992).

Chinta et al. investigated the effects of cross-coupling forces using current control, where the nonlinear force to displacement and the nonlinear force to coil current characteristics are additionally active, (Chinta, et al., 1996). Again an AMB system with a single-mass rotor excited by unbalance forces is considered. They used the tool of numerical simulation method. Quasiperiodic and period-2 solutions for the rotor vibration were found.

Beside the above discussed references several authors applied the classical methods of harmonic balance, describing function and perturbation theory to autonomous or non-autonomous AMB systems, see (Hoffmann, et al., 1997; Knight, et al., 1993; Nataraj, 1995; Sinha, 1990). Moreover, stable limit cycles as response to speed synchronous unbalance excitation were found by the tool of numerical simulation, see (Haferl, Springer, 1991; Jeong, et al., 1994; Knight, Ecker, 1996; Knight, et al., 1993; Satoh, et al., 1990; Springer, et al., 1990).

This paper discusses an AMB-supported single-mass rotor with speed synchronous unbalance excitation. The mathematical model includes the nonlinear force to displacement and force to coil current relationship. Beside possible saturation effects, see (Springer, et al., 1998), this is the most important nonlinearity in the case of high vibration amplitudes compared with the air gap length. The investigation of this relatively simple model and the complete understanding of its dynamical behaviour is necessary for a successful application of the path-following method and for a correct interpretation of calculated solutions for more advanced mathematical models. Therefore, the discussed model should be seen as a basis for further investigations.

AMB SYSTEM MODEL

Magnetic Force Model

The calculation of the magnetic forces generated by the AMB-actuators is based on the common used, one-dimensional model for the magnetic flux, see (Schweitzer, et al., 1993).

Leakage and fringing effects, hysteresis and saturation of the magnetic material are neglected. The permeability in the iron paths is considered to be very high compared with the permeability of the air paths. Thus, the mathematical formulation of the magnetic force for one actuator can be written as

$$f = k\frac{i^2}{(2g)^2}, \tag{1}$$

where k is a constant value depending on the actuator properties, i is the coil current in the actuator and g is the air gap length between rotor and stator.

Magnetic Bearing Model

Figure 1 shows a schematic diagram of an active magnetic bearing viewed along the axis of the shaft, which is plotted for the center position ($x = 0, y = 0, g = g_0$).

The discussed magnetic bearing consists of two pairs of orthogonally oriented electromagnets. The magnet pairs are controlled independently. Any coupling effects between both directions are neglected.

In each magnet pair one collocated displacement sensor measures the rotor position in the $x-$ or $y-$direction, respectively. The displacement signal is the input for the PD-current controller. According to the output of the controller the amplifier supplies the voltage to produce the appropriate magnetic force in the actuator.

In order to achieve a stable, damped system a bias current i_b, which has a static, predefined value, is supplied in each actuator and a control current, which corresponds to the controller output, is superimposed. It is very common to apply a so-called 'differential control', which means that one magnetic actuator input consists of the bias current plus the control current, while the input of the opposite actuator consists of the bias current minus the control current. Thus, the coil currents in the actuators acting in $x-$ and $y-$directions, respectively, are

$$\begin{aligned} i_{x,+} &= i_b - G_P x - G_D \dot{x} \\ i_{x,-} &= i_b + G_P x + G_D \dot{x} \\ \\ i_{y,+} &= i_b - G_P y - G_D \dot{y} \\ i_{y,-} &= i_b + G_P y + G_D \dot{y}, \end{aligned} \tag{2}$$

where G_P is the proportional feedback gain and G_D is the differential feedback gain. The subscripts + and - identify the actuators on the positive and on the negative axes, respectively, see Figure 1. In the special case, when the bearing does not carry a steady lateral load, the bias current i_b will be equal in all actuators. This is assumed in the following.

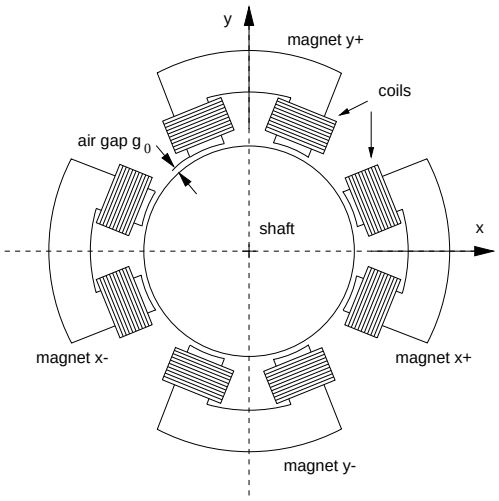

Figure 1. SCHEMATIC OF AN ACTIVE MAGNETIC BEARING WITH SHAFT IN CENTER POSITION.

Rotor Model

The rotor is represented as a lumped mass with two degrees of freedom supported by two opposed magnetic actuators in both directions, see Figure 1. The rotor is excited by speed synchronous unbalance forces, which are caused by the mass imbalance eccentricity e. Thus, the equations of motion have the form

$$\begin{aligned} m\ddot{x} &= f_{x,mag} + me\omega^2\cos(\omega t) \\ m\ddot{y} &= f_{y,mag} + me\omega^2\sin(\omega t), \end{aligned} \tag{3}$$

where m is the mass of the rotor, $f_{x,mag}$ is the resulting magnetic force exerted to the rotor by both actuators in the $x-$direction and $f_{y,mag}$ is the resulting magnetic force exerted to the rotor by both actuators in the $y-$direction. Furthermore, ω is the angular velocity of the rotor and t is the physical time.

Equations of Motion

A dimensionless formulation for the equations of motion, can be introduced by the following dimensionless variables

$$\begin{aligned} X &= \frac{x}{g_0} & G_{PN} &= \frac{G_P g_0}{i_b} \\ Y &= \frac{y}{g_0} & G_{DN} &= \frac{G_D \omega_0 g_0}{i_b} \\ E &= \frac{e}{g_0} & \Omega &= \frac{\omega}{\omega_0} \\ \tau &= \frac{\omega}{2\pi} t, \end{aligned} \tag{4}$$

where g_0 is the air gap length between the rotor and the stator at the rotor center position. This definition of a dimensionless time τ maps one excitation period into the interval $[0,1]$, which is useful for the formulation of the boundary value problem, see section 'Numerical Solution Method'. The natural frequency of the linearized system is given by

$$\omega_0 = \sqrt{k\frac{(G_{PN}-1)i_b^2}{mg_0^3}}. \tag{5}$$

The damping ratio ζ can be written as

$$\zeta = \frac{G_{DN}}{2(G_{PN}-1)}. \tag{6}$$

Finally, the dimensionless equations of motion have the form

$$\begin{aligned} X'' &= \left(\frac{2\pi}{\Omega}\right)^2 \left[\frac{F_{x,+}-F_{x-}}{G_{PN}-1} + E\Omega^2\cos(2\pi\tau)\right] \\ Y'' &= \left(\frac{2\pi}{\Omega}\right)^2 \left[\frac{F_{y,+}-F_{y-}}{G_{PN}-1} + E\Omega^2\sin(2\pi\tau)\right], \end{aligned} \tag{7}$$

where the primes denote the derivatives with respect to the dimensionless time τ and

$$\begin{aligned} F_{x,+} &= \frac{(1-G_{PN}X-G_{DN}\frac{\Omega}{2\pi}X')^2}{4(1-X)^2} \\ F_{x,-} &= \frac{(1+G_{PN}X+G_{DN}\frac{\Omega}{2\pi}X')^2}{4(1+X)^2} \\ F_{y,+} &= \frac{(1-G_{PN}Y-G_{DN}\frac{\Omega}{2\pi}Y')^2}{4(1-Y)^2} \\ F_{y,-} &= \frac{(1+G_{PN}Y+G_{DN}\frac{\Omega}{2\pi}Y')^2}{4(1+Y)^2}, \end{aligned} \tag{8}$$

being the dimensionless forces

$$F_i = f_i\frac{g_0^2}{ki_b^2} \tag{9}$$

with $i = x,y$.

Magnetic Force Characteristics

Considering the quasistatic case, with no differential feedback being active, the dimensionless magnetic forces produced by the magnet pairs are given by

$$F_x = \frac{(1-G_{PN}X)^2}{4(1-X)^2} - \frac{(1+G_{PN}X)^2}{4(1+X)^2}$$
$$F_y = \frac{(1-G_{PN}Y)^2}{4(1-Y)^2} - \frac{(1+G_{PN}Y)^2}{4(1+Y)^2}, \tag{10}$$

or

$$F_x = (G_{PN}-1)\frac{X\left(G_{PN}X^2-1\right)}{\left(1-X^2\right)^2}$$
$$F_y = (G_{PN}-1)\frac{Y\left(G_{PN}Y^2-1\right)}{\left(1-Y^2\right)^2}. \tag{11}$$

In Figure 2 the force function in $x-$direction $F_x(X)$ is plotted for various values of the proportional feedback gain G_{PN}, characterized by different colors in the plot. Since

$$\left.\frac{dF_x}{dX}\right|_{X=0} = -(G_{PN}-1) \tag{12}$$

holds, there is a lower limit for G_{PN}. The forces F_x and F_y are defined as restoring forces exerted to the rotor. Therefore, a positive linear stiffness for the center position of the rotor requires

$$G_{PN} \geq 1.0, \tag{13}$$

see also Eq. (5).

Moreover, Figure 2 shows a strong nonlinear behaviour of the magnetic force for high values of the rotor displacement. The direction of the force is even reversed if

$$|X| > \frac{1}{\sqrt{G_{PN}}}. \tag{14}$$

A higher value for G_{PN} enables a higher linear stiffness for the center position and a higher maximum of the restoring force. On the contrary the approximately linear region in the vicinity of the center position and the region for a positive restoring force are smaller for higher values of G_{PN}. Summing up, this plot shows that the autonomous, conservative system possesses only a well defined region, where periodic solutions are possible.

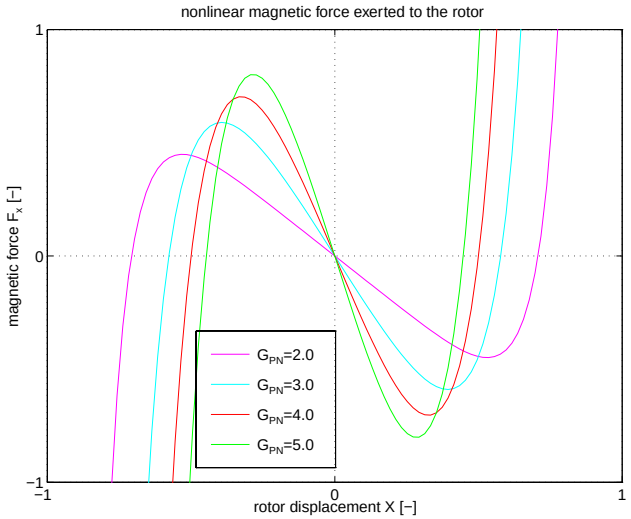

Figure 2. NONLINEAR MAGNETIC FORCE EXERTED TO THE ROTOR WITHOUT DIFFERENTIAL FEEDBACK. THE PROPORTIONAL FEEDBACK G_{PN} IS VARIED FROM 2.0 TO 5.0.

Model Limitations

The complete understanding of the discussed model of the AMB system is necessary for a correct interpretation of system responses of more sophisticated models to be investigated in future works. This simple model only contains the nonlinear force to air gap and force to coil current relationships. Saturation effects of the magnetic material, the current controller and the amplifier are neglected. No fringing and no leakage of the magnetic flux is considered. Magnetic flux paths coupling different magnets are not modeled. Therefore, flux densities in different magnets are calculated from independent magnetic circuits. There is no modeling of the inductance of the coils, instead the coil current is considered to follow the applied voltage instantaneously. Any coupling between different coordinate directions is not modeled. The system is completely symmetrical because no lateral static load is considered.

NUMERICAL SOLUTION METHOD

The presented mathematical model has already been discussed by several authors with the tool of numerical simulation. However, a simulation approach, based in the Initial Value Problem (IVP) has the disadvantage that a sufficiently large number of transient cycles must be allowed to decay before a steady-state response is reached. This makes this approach cumbersome and slow, especially near stability limits of the system. Furthermore, unstable solutions of limit cycles cannot be calculated by this method. A positive aspect of the simulation approach via IVP is that it is not restricted to periodic solutions. Any kind of quasi-

periodic or even chaotic solutions can be found by the simulation approach.

A second widely used approach is the harmonic balance method, which is rather an analytical than a numerical approximation. It has the advantage that both stable and unstable solutions can be obtained. However, the method does not yield stability characteristics. Since an approximation of the original system is solved, there is always the question about the validity of the results obtained by this method.

In this investigation the numerical simulation method is an additional tool only, primarily used for verification and for calculation of time plots. It is obvious that the steady-state response of the system is basically periodic with the period T of one rotor revolution. Therefore, numerical integration is used, but formulated as a Boundary Value Problem (BVP). By employing periodic boundary conditions $z(0) = z(T)$ and solving the BVP numerically by an appropriate method any kind of stable or unstable periodic solutions can be calculated. To track solutions for a certain parameter variable, in our case the exciting unbalance frequency Ω, a smart continuation (path-following) method has to be used. This becomes very important if turning points occur during the continuation process.

The following results were obtained using the subroutine collection BIFPACK, see (Seydel, 1996). BIFPACK provides a multiple shooting routine to solve boundary value problems, it possesses a sophisticated continuation algorithm and it can investigate the stability of a periodic solution, as outlined before. Beside other useful features the package offers a branch switching option to calculate new starting points on emanating solutions near a bifurcation.

NUMERICAL RESULTS

Solving the BVP as mentioned for the non-autonomous system with speed synchronous unbalance excitation, bifurcation diagrams can be produced with the rotor speed Ω as the chosen bifurcation parameter. Numerical simulation is used for verification and interpretation of the obtained stable or unstable periodic solutions.

In the following, system responses are discussed for certain parameter values in order to show only the most interesting results of this research. Since a fully symmetrical problem is discussed, all diagrams are valid for both direction x and y. Figure 3 shows the steady-state amplitudes of the rotor vibration in $x-$ or $y-$direction, respectively, versus the dimensionless excitation frequency Ω. Stable periodic solutions are represented by green lines, unstable periodic solutions by red lines. All solutions are calculated for $G_{PN} = 3.0$ and $E = 0.35$. The differential feedback gain G_{DN} is varied from 3.27 to 1.34.

Considering a well damped system with $G_{DN} = 3.27$ i.e. $\zeta = 0.818$ and sweeping from low to high values of the excitation frequency, first the system behaves approximately linear until the

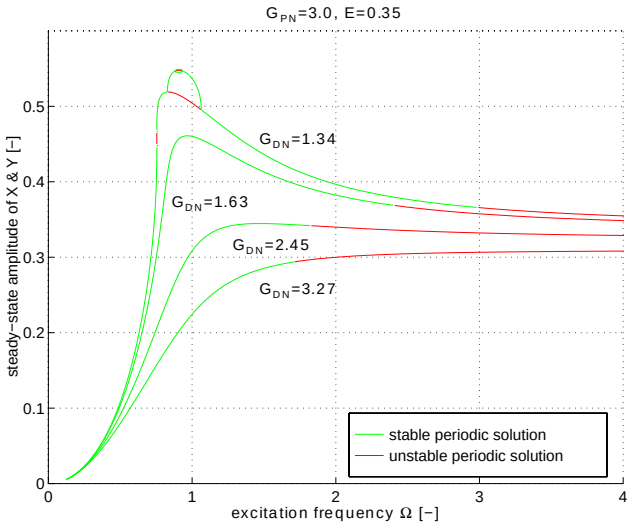

Figure 3. AMB SYSTEM RESPONSE FOR THE PARAMETER VALUES $G_{PN} = 3.0$ AND $E = 0.35$. G_{DN} IS VARIED FROM 3.27 TO 1.34.

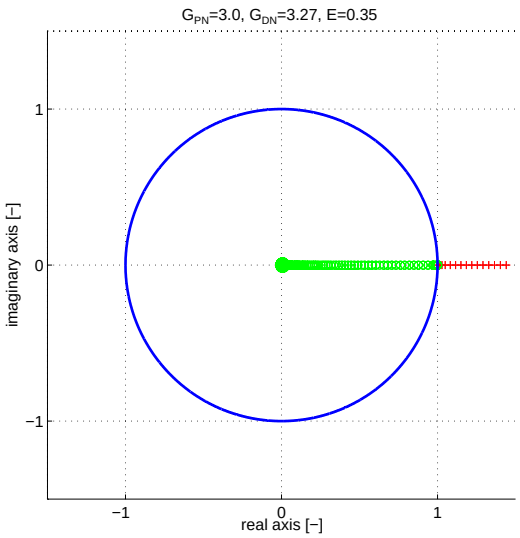

Figure 4. EIGENVALUES OF THE MONODROMY MATRIX FOR THE PARAMETER SET $G_{PN} = 3.0$, $G_{DN} = 3.27$ AND $E = 0.35$. Ω IS VARIED FROM 0.1 TO 1.87.

stability of the periodic solutions changes at $\Omega = 1.71$. Beyond that threshold a stable periodic solution could not be obtained any more. The system becomes globally unstable. As Figure 3 shows, this effect appears for all plotted parameter sets.

At the threshold $\Omega = 1.71$ one of the eigenvalues of the monodromy matrix crosses the unit circle on the positive real axis. Figure 4 shows the development of the eigenvalues with respect to the bifurcation parameter Ω in the range $\Omega = 0.1$ to $\Omega = 1.87$.

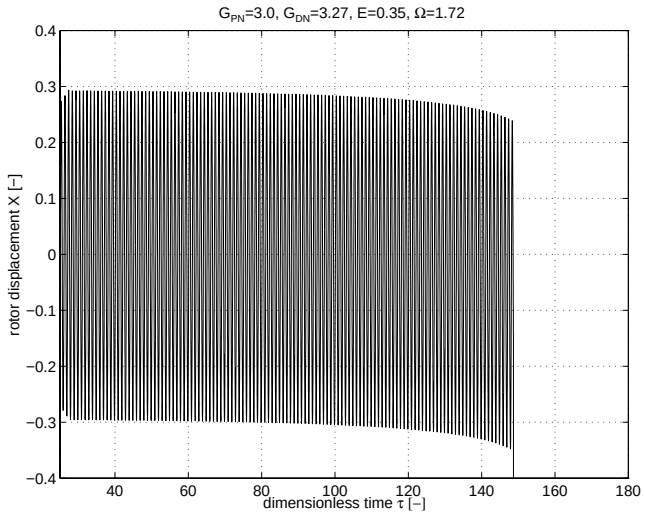

Figure 5. ROTOR VIBRATION IN TERMS OF DIMENSIONLESS TIME τ FOR THE PARAMETER SET $G_{PN} = 3.0$, $G_{DN} = 3.27$, $E = 0.35$ AND $\Omega = 1.72$.

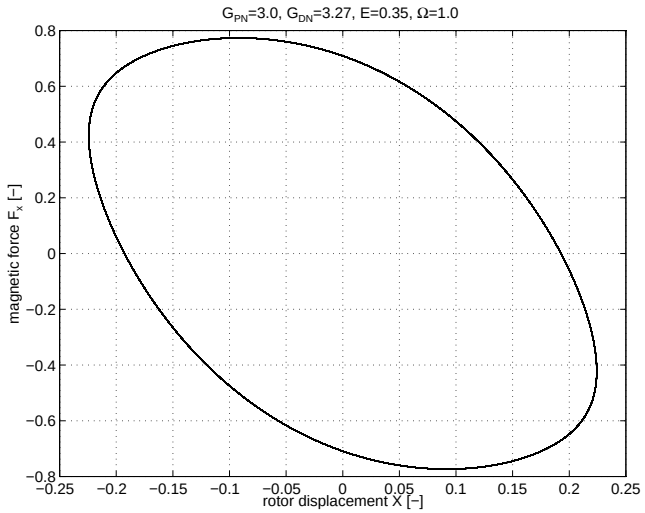

Figure 6. MAGNETIC FORCE IN TERMS OF ROTOR DISPLACEMENT FOR THE PARAMETER SET $G_{PN} = 3.0$, $G_{DN} = 3.27$, $E = 0.35$ AND $\Omega = 1.0$.

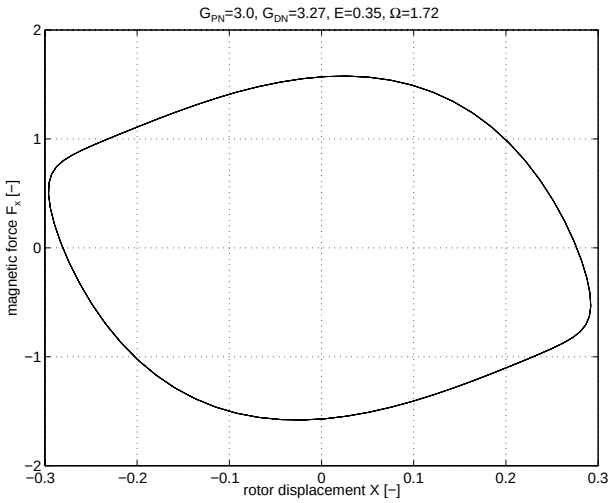

Figure 7. MAGNETIC FORCE IN TERMS OF ROTOR DISPLACEMENT FOR THE PARAMETER SET $G_{PN} = 3.0$, $G_{DN} = 3.27$, $E = 0.35$ AND $\Omega = 1.72$.

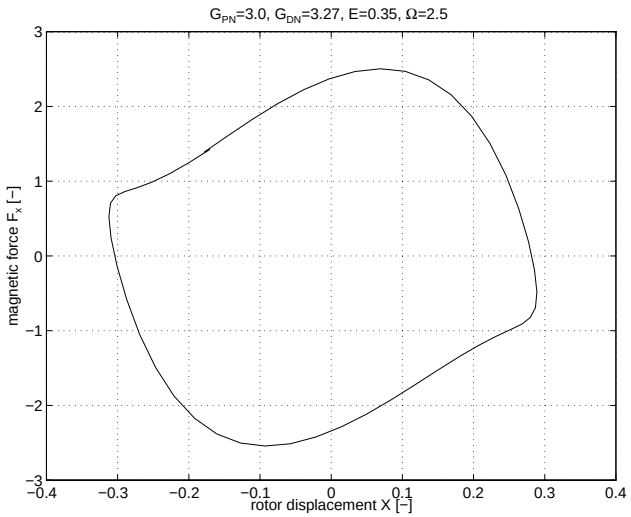

Figure 8. MAGNETIC FORCE IN TERMS OF ROTOR DISPLACEMENT FOR THE PARAMETER SET $G_{PN} = 3.0$, $G_{DN} = 3.27$, $E = 0.35$ AND $\Omega = 2.5$.

This threshold for stable solutions is sensitive with respect to the differential feedback gain G_{DN}. For higher values of G_{DN} the unstable branch extends to lower values of the excitation frequency Ω.

Choosing appropriate initial values for the system variables at the beginning of the unstable branch and solving the IVP gives more insight into that phenomenon. The calculated time plot is shown in Figure 5. Although the peak to peak value of the rotor vibration is nearly unchanged, there is no well defined center of the rotor orbit any more. As a result the rotor drifts away causing a failure of the AMB system.

Figures 6, 7 and 8 show the magnetic forces in terms of the rotor displacements calculated with the above mentioned IVP. Figure 6 corresponds to a stable solution at $\Omega = 1.0$, Figure 7 is obtained for the threshold value $\Omega = 1.72$ and Figure 8 shows the situation for the unstable branch at $\Omega = 2.5$. The enclosed area

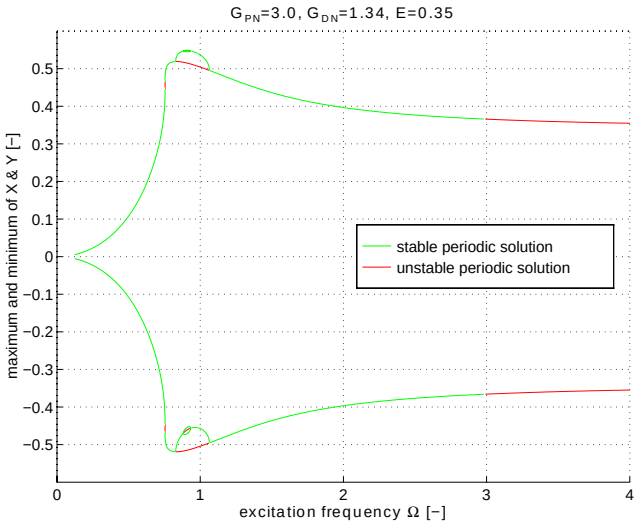

Figure 9. AMB SYSTEM RESPONSE FOR THE PARAMETER VALUES $G_{PN} = 3.0$, $G_{DN} = 1.34$ AND $E = 0.35$. THE PLOT SHOWS MAXIMUM AND MINIMUM OF THE UNSYMMETRIC PERIODIC SOLUTION. MAGNIFICATIONS ARE SHOWN IN FIGURES 10 AND 11.

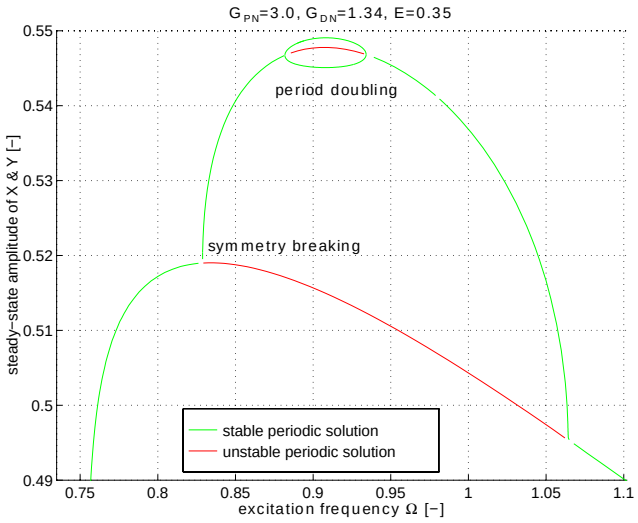

Figure 10. AMB SYSTEM RESPONSE FOR THE PARAMETER VALUES $G_{PN} = 3.0$, $G_{DN} = 1.34$ AND $E = 0.35$. DETAIL OF FIGURE 9.

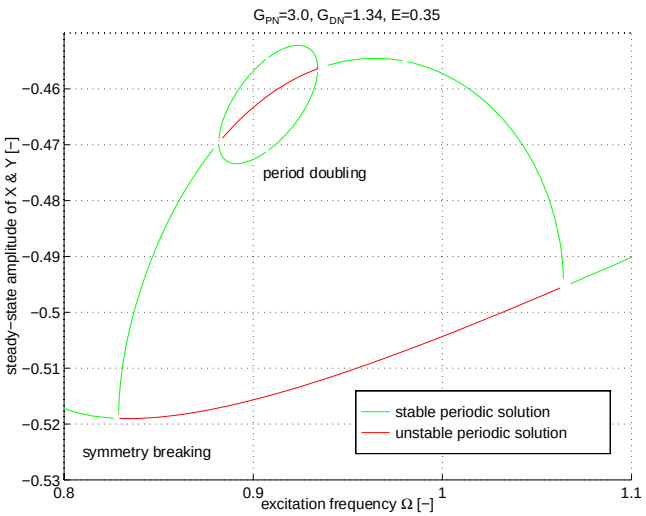

Figure 11. AMB SYSTEM RESPONSE FOR THE PARAMETER VALUES $G_{PN} = 3.0$, $G_{DN} = 1.34$ AND $E = 0.35$. DETAIL OF FIGURE 9.

within the closed curve is a measure for the dissipated energy (in the sense of a differential control feedback) during one excitation period. Comparing Figures 6, 7 and 8, it can be easily seen that the ratio between the enclosed areas in the quadrants I and II or quadrants III and IV, respectively, increases with increasing rotor speed. As result, the effect of the mechanism of this stability loss can be compared with the loss of stiffness in a linear system.

A decrease in the differential feedback results in higher steady-state amplitudes of the rotor vibrations, see Figure 3. The shift of the maxima of the steady-state amplitudes to lower frequencies with decreasing differential gain values G_{DN} is caused by the softening spring characteristic of the system. Figure 3 shows that for $G_{DN} = 1.34$ even two turning points with unstable solution in between are found.

Looking at the system response for $G_{DN} = 1.34$, another nonlinear phenomenon occurs. At $\Omega = 0.83$ symmetry breaking is dedected, as shown in Figures 9, 10 and 11. One of the eigenvalues of the monodromy matrix crosses the unit circle on the positive real axis, see Figure 12. The symmetric solution becomes unstable at the bifurcation point, where a stable, unsymmetric solution emanates. Since the maximum and minimum values of the rotor vibrations are not equal in the case of the unsymmetric solution, there are four possible stable rotor orbits which are symmetric with respect to the $x-$ or $y-$axis, respectively. In Figure 9 the rotor vibration amplitude is limited between two plotted lines for maximum and minimum, to give a better insight into the phenomenon. A coexisting second unsymmetric solution can be found symmetric to the abscissa.

Figure 13 shows the unstable symmetric (red line) and the stable unsymmetric (green line) rotor orbit for $\Omega = 0.98$. It is worth to note that the symmetric periodic solution contains superharmonic components of the third order, which are responsible for the noncircular shape of the orbit. The amplitude of the rotor vibration is limited by the air gap between the rotor and the stator. This is visualized by the blue circle. It should be mentioned that these nonlinear effects are found for vibration amplitudes already at half of the air gap length, which may become important for practical applications.

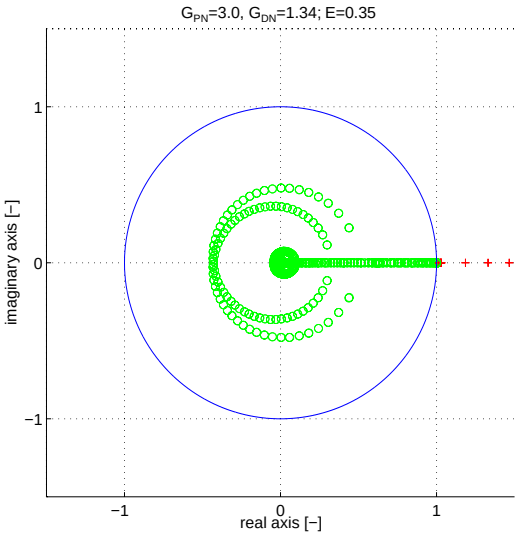

Figure 12. EIGENVALUES OF THE MONODROMY MATRIX FOR THE PARAMETER SET $G_{PN} = 3.0$, $G_{DN} = 1.34$ AND $E = 0.35$. Ω IS VARIED FROM 0.1 TO 0.85.

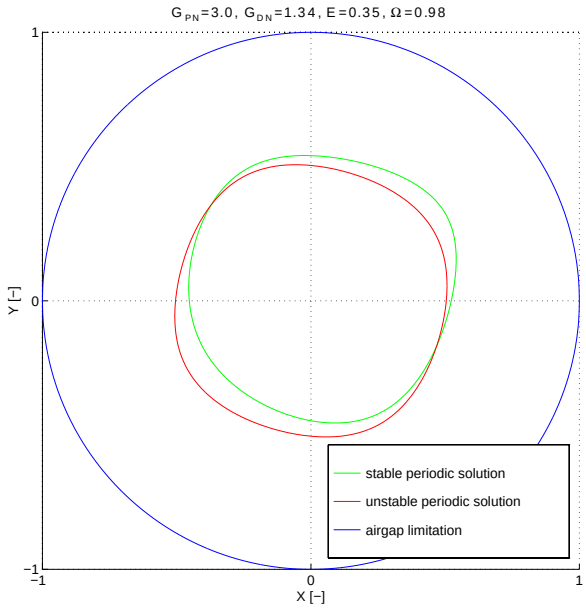

Figure 13. STABLE UNSYMMETRIC SOLUTION AND UNSTABLE SYMMETRIC SOLUTION FOR THE PARAMETER SET $G_{PN} = 3.0$, $G_{DN} = 1.34$, $E = 0.35$ AND $\Omega = 0.98$.

For low values of the differential feedback gain G_{DN} even a flip-bifurcation occurs, see Figures 10 and 11. At the bifurcation point the unsymmetric solution becomes unstable. A stable unsymmetric solution with doubled period emanates. One of four possible rotor orbits is shown in Figure 14. At $\Omega = 0.88$ one of the eigenvalues of the monodromy matrix crosses the unit circle on the negative real axis, see Figure 15.

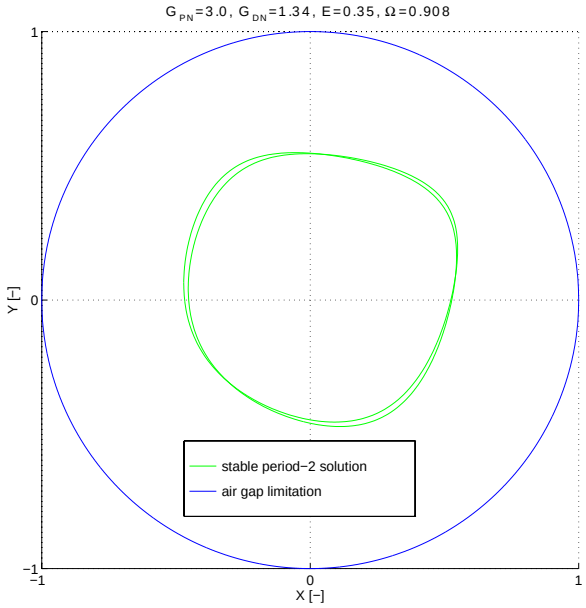

Figure 14. STABLE UNSYMMETRIC SOLUTION WITH PERIOD 2 FOR THE PARAMETER SET $G_{PN} = 3.0$, $G_{DN} = 1.34$, $E = 0.35$ AND $\Omega = 0.908$.

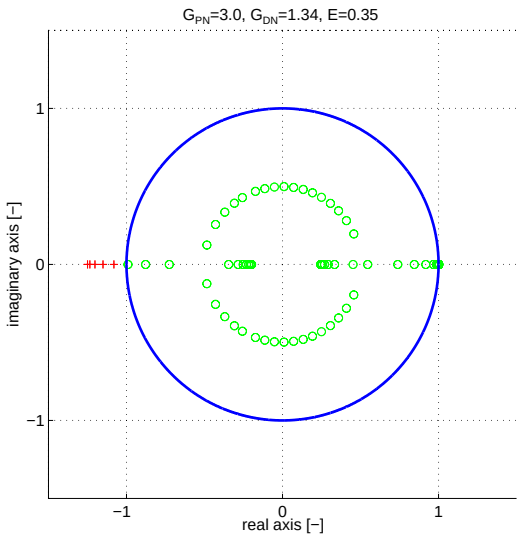

Figure 15. EIGENVALUES OF THE MONODROMY MATRIX FOR THE PARAMETER SET $G_{PN} = 3.0$, $G_{DN} = 1.34$ AND $E = 0.35$. Ω IS VARIED FROM 0.83 TO 0.9.

CONCLUSION

Even a simple model of an AMB system shows important nonlinear phenomena if nonlinear force to displacement and force to current characteristics are included in the analysis. Numerical results obtained by solving a boundary value problem combined with the path following method are presented. Stable and unstable periodic solutions are calculated. For specific parameter sets symmetry breaking and period doubling may occur. It is shown that important phenomena exist in AMB systems not predictable with linear methods. Further investigations will be done in the future to discuss more sophisticated models, including saturation effects, modeling of coil inductance, geometric coupling effects and static preload for example.

ACKNOWLEDGMENT

The authors gratefully acknowledge the support of this project by the Austrian science foundation 'Fonds zur Förderung der wissenschaftlichen Forschung (FWF)'.

REFERENCES

Chinta, M., Palazzolo, A.B., Kascak, A., *Quasiperiodic Vibration of a Rotor in a Magnetic Bearing with Geometric Coupling*, Proc. of 5th Int. Symp. on Magnetic Bearings, Kanazawa, Japan, 1996.

Ecker, H., Knight, J.D., Wu, L., *Nonlinear Dynamic Simulation of an Active Magnetic Bearing System with Non-symmetric Coordinate Coupling Forces*, Proc. of Int. Gas Turbine & Aeroengine Congress & Exhibition, Orlando, Florida, ASME Conf. paper No. 97-GT-113, 1997.

Haferl, A., Springer, H., *Simulation von Magnetisierungsprozessen in Magnetlagern*, Proc. of 7. Symp. Simulationstechnik, ASVM-Tagung in Hagen, Verlag Vieweg, 1991.

Hebbale, K.V., *A Theoretical Model for the Study of Nonlinear Dynamics of Magnetic Bearings*, Ph.D. thesis, Cornell University, 1985.

Hebbale, K.V., Taylor, D.L., *Nonlinear Dynamics of Attractive Magnetic Bearings*, Proc. of the Workshop on Rotordynamic Instability Problems in High-Performance Turbomachinery, Texas A&M-Univ., NASA-Conf. Publ. No. 2443, 1986.

Hoffmann, K.-J., Laier, D., Markert, R., *Nonlinear Control of Magnetically Supported Rotors*, Proc. of MAG'97 - Industrial Conference and Exhibition on Magnetic Bearings, Alexandria, VA, 1997.

Jeong, H.S., Kim, C.S., Lee, C.W., *Modelling and Control of Cone Shaped Active Magnetic Bearing Systems*, Proc. of 4th Int. Symp. on Magnetic Bearings, ETH-Zürich, 1994.

Knight, J.D., Ecker, H., *Simulation of Nonlinear Dynamics in Magnetic Bearings with Coordinate Coupling*, Proc. of Summer Computer Simulation Conf., Portland, Oregon, 1996.

Knight, J., Walsh, T., Virgin L., *Dynamic Analysis of a Magnetic Bearing System with Flux Control*, Proc. of 2nd Int. Symp. on Magnetic Suspension Technology, Seattle, WA, 1993.

Knight, J.D., Xia, Z., McCaul, E.B., *Forces in Magnetic Journal Bearings: Nonlinear Computation and Experimental Measurement*, Proc. of 3rd Int. Symp. on Magnetic Bearings, Alexandria, VA, 1992.

Lang, O., Wassermann, J., Springer, H., *Adaptive Vibration Control of a Rigid Rotor supported by Active Magnetic Bearings*, Proc. of Int. Gas Turbine and Aeroengine Congress and Exposition, Houston, Texas, 1995.

Mohamed, A.M., Emad, F.P., *Nonlinear Oscillations in Magnetic Bearing Systems*, IEEE Transactions on Automatic Control, Vol. 38, No.8, 1993.

Moser, F., *Stabilität und Verzweigungsverhalten eines nichtlinearen Rotor-Lager-Systems*, Ph.D. thesis, Vienna University of Technology, 1993.

Nataraj, C., *Nonlinear Analysis of a Rigid Rotor on Magnetic Bearings*, Proc. of Int. Gas Turbine and Aeroengine Congress and Exposition, Houston, ASME Conf. paper No. 95-GT-204, 1995.

Satoh, I., Murakama, C., Nakajima, A., Kanemitsu, Y., *A Self-Excited Vibration of Magnetic Bearing Systems with Flexible Structure*, Proc. of 2nd Int. Symp. on Magnetic Bearings, Tokyo, 1990.

Schweitzer, G., Traxler, A., Bleuler, H., *Magnetlager, Grundlagen, Eigenschaften und Anwendungen berührungsfreier, elektromagnetischer Lager*, Springer Verlag, Berlin, 1993.

Seydel R., *BifPack, a Program Package for Continuation, Bifurcation and Stability Analysis*, Program documentation, University of Ulm, Germany, 1996.

Sinha, A., *On the Design of Magnetic Suspension Systems*, Proc. of Gas Turbine and Aeroengine Congress and Exposition, Belgium, ASME Conf. paper No. 90-GT-239, 1990.

Springer, H., Maslen, E.H., Humphris, R.H., *Nonlinear Hysteresis Effects in Electromagnetic Bearings*, Proc. of 3rd Int. Conf. on Rotordynamics, Lyon, (Ed.du CNRS), 1990.

Springer, H., Schlager, G., Platter T., *A Nonlinear Simulation Model for Active Magnetic Bearing Actuators*, Proc. of 6th Int. Symp. on Magnetic Bearings, MIT Cambridge, MA, 1998.

Troger, H., Steindl, A., *Nonlinear Stability and Bifurcation Theory*, Springer Verlag, Wien - New York, 1991.

Virgin, L., Walsh, T.F., Knight, J.D., *Nonlinear Behavior of a Magnetic Bearing System*, Proc. of Int. Gas Turbine and Aeroengine Congress and Exposition, The Hague, Netherlands, ASME Conf. paper No. 94-GT-341, 1994.

Wang, H., Wu, Z., Niu, X., *Dynamic Bifurcations of Active Magnetic Bearings Rotor Systems*, Proc. of 4th Int. Symp. on Magnetic Bearings, ETH-Zürich, 1994.